RESEARCH ACTIVITIES V
Department of Applied Molecular Science

V-A Synthesis of Chiral Molecule-Based Magnets

Construction of molecule-based magnetic materials, which have additional properties such as conductivity or photo reactivity, is now becoming a challenging target. Specific goals aimed for these molecule-based magnets include: i) the ability to design the molecular building blocks and to organize them in the solid for desired dimensionality, ii) the optical transparency. The physical characteristic of current interest involves optical properties, particularly with respect to natural optical activity. When a magnet has optical transparency and chiral structure, the magnetic structure of crystal expects to be a chiral spin structure. These magnets will show an asymmetric magnetic anisotropy and magneto-chiral dichroism. This category of materials don't only have scientific interest but also have the possibility for use in new devices. When we construct chiral molecule-based magnets, chirality must be controlled not only in the molecular structure, but in the entire crystal structure. As a consequence of this difficulty, only few examples of this type of magnet exist. Up to the present reported chiral magnets have low dimensional magnetic structures, the magnetic ordering temperatures are below 10 K. To afford a high-T_C magnet, dimensionality of magnetic structure must be extended in two or three dimension. When we introduce magnetic bricks, which have more than three connections for the construction of magnets, we can expect to make two or three-dimensional magnets. To make high dimensionality molecule-based magnets, we recently discovered using cyano bridged complex with chiral organic ligands.

V-A-1 A Novel Two-Dimensional Chiral Complex; [Cu-II(*R*)-pn]$_2$[Ni-II(CN)$_4$]$_2$·H$_2$O ((*R*)-pn = (*R*)-1,2-Diaminopropane)

IMAI, Hiroyuki; INOUE, Katsuya; OHBA, Masaaki[1]; OKAWA, Hisashi[1]; KIKUCHI, Koichi[2]
([1]Kyushu Univ.; [2]IMS and Tokyo Metropolitan Univ.)

[*Synth. Met.* **137**, 919–920 (2003)]

The synthesis, single crystal X-ray structures and magnetic properties of a new two-dimensional chiral complex; [Cu-II(*R*)-pn]$_2$[Ni-II(CN)$_4$]$_2$·H$_2$O ((*R*)-pn = (*R*)-1,2-diaminopropane), are described. Blue plate crystals of [Cu-II(*R*)-pn]$_2$[Ni-II(CN)$_4$]$_2$·H$_2$O were obtained by the reaction between [Cu(*R*)-pn](SO$_4$) and K$_2$[Ni(CN)$_4$] in H$_2$O-EtOH(1:1). The structures consist of a two-dimensional cyano-metal network as shown in Figure 1 and 2. The temperature dependence of χT is shown in Figure 3. At low temperature χT decreases with lowering temperature. This tendency indicates a weak antiferromagnetic interaction dominates between copper ions. The magnetic susceptibility of this crystals can be reproduced by Curie-Weiss law with the parameters of C = 0.849 emu K mol^{-1} (g = 2.2) and θ = –1.27 K.

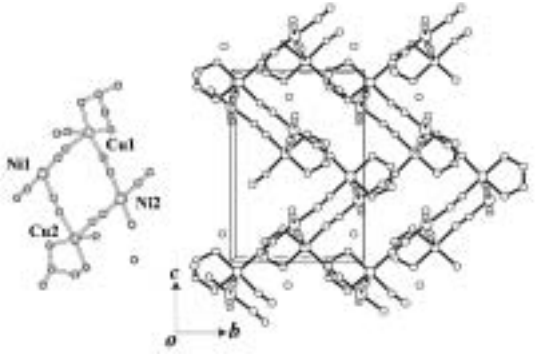

Figure 1. The asymmetric unit of [Cu^{II}(*R*)-pn]$_2$[Ni^{II}(CN)$_4$]$_2$ H$_2$O and the two-dimensional chiral network in the *bc*-plane.

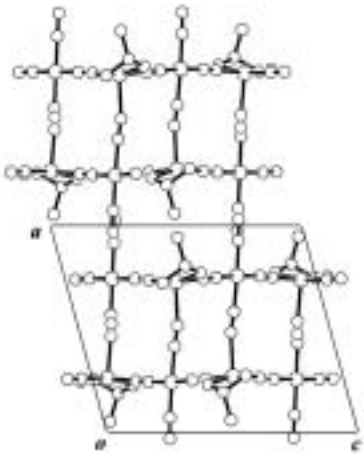

Figure 2. The side view of the two-dimensional sheet along *b*-axis.

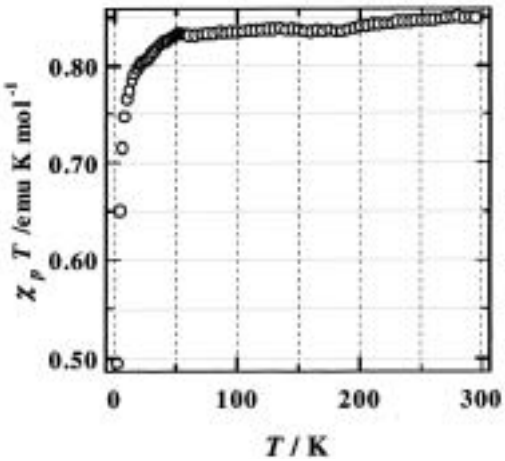

Figure 3. The temperature dependence of the χT.

V-B Hydrothermal Synthesis of Molecule-Based Magnets

Coordination polymers are attracting much interest due to the strength and rigidity of the extended lattices for gas absorption and intercalation and for the connectivity between magnetic ions in designing molecule-based magnets. They belong to a subset of organic-inorganic hybrid materials, and usually employ a central metal ion and a multitopic organic ligands or a coordination complex having ambidentate ligands, such as cyanide and oxalate. In some cases, other organic ligands are used to control the dimensionality or structure. The choice of the metals and of the ligands depends on the desired properties. On the one hand, there is strong interest by scientists studying catalysis and the absorption of gases originating from the possibility of creating structures with cavities, channels or pores and, consequently, large surface areas. On the other hand, there is increasing interest from magneto-chemists due principally to the realization of organizing the magnetic orbitals of the moment carriers to favor a particular magnetic ground state. The field of coordination polymers based on organic radicals is a very active area, indeed. Several ground states have been established and a clear molecular-orbital picture to explain the observations is emerging. For the realizing strong magnetic interaction, it is better to use simple and small organic ligands, such as cyanide or carboxylate ions. The metal complexes with such ligands are usually less solvability. The thermal synthesis is powerful method to make large single crystals for such complexes.

V-B-1 Synthesis and Characterization of One-Dimensional Mixed-Spin Cobalt(II) Metamagnet

OKA, Yoshimi; KUMAGAI, Hitoshi; INOUE, Katsuya

The hydrothermal synthesis, single crystal X-ray analysis and magnetic properties of a one-dimensional mixed-spin Co^{II} Metamagnet, $[Co_4(phcina)_6(OH)_2(H_2O)_4]\cdot 2H_2O$ (phcina = alpha-phenylcinnamate), is described. Pink needle crystals of $[Co_4(phcina)_6(OH)_2(H_2O)_4]\cdot 2H_2O$ was obtained at 120 °C. The x-ray structure analysis of **1** revealed the formation of 1-D chain along the *c*-crystal axis. (Figure 1 and 2). The asymmetric unit consists of two distorted octahedral Co^{II} ions (Co(1), Co(3)) and two octahedral Co^{II} ions (Co(2), Co(4)). Co(2) and Co(4) exhibit octahedral geometry comprising of three oxygen atoms of phcina ligands, one hydroxide and two waters. The O–Co–O bond angles in the $\{CoO_6\}$ octahedral site range from 81.37(8) ° to 98.18(10) ° and bond distances range from 2.029(2) to 2.163(3) Å (*av*. 2.10 Å). These values are similar to that found in octahedral Co^{II}(HS) complexes. In contrast, Co(1) and Co(3) exhibit distorted octahedral geometry, pseudo C_{4v} symmetry comprising of three oxygen atoms of phcina ligands, two hydroxides and one water. Co(1) has O(2), O(7), O(9) and O(15) in the basal plane and these O–Co(1)–O angles range from 82.16(10) ° to 94.37(10) °. These configurations are similar that found in Co^{II}(LS) complexes. The nearest intermetallic separation between Co···Co along*b*-axis is 3.095(2) Å and that along *a*-or *c*-axis is more than 14.406(4) Å. Figure 3 shows the temperature dependence of the magnetic susceptibility, the product of susceptibility and temperature and inverse susceptibility. The χT value is 9.87 emu K mol^{-1} at 300 K and reaches a local minimum at 35 K (7.18 emu K mol^{-1}) and then rapidly increases. The effective magnetic moment (μ_{eff}) per four cobalt ions is 9.87 μ_B at room temperature which is consistent with that expected for four Co^{II}(HS) ions. It is indicative that the value 7.58 μ_B of μ_{eff} at 35 K is assigned to two distorted octahedral Co^{II}(LS) and two octahedral Co^{II}(HS) ions, this complex shows gradual spin-crossover behavior of Co^{II} with C_{4v} symmetry and orbital contribution through spin-orbit coupling of octahedral Co^{II} ions as temperature increases. High-spin Co^{II} ions and low-spin Co^{II} ions interact ferrimagnetically and ferrimagnetic chains interact antiferromagnetically below T_N = 5.5 K. (Figure 4)

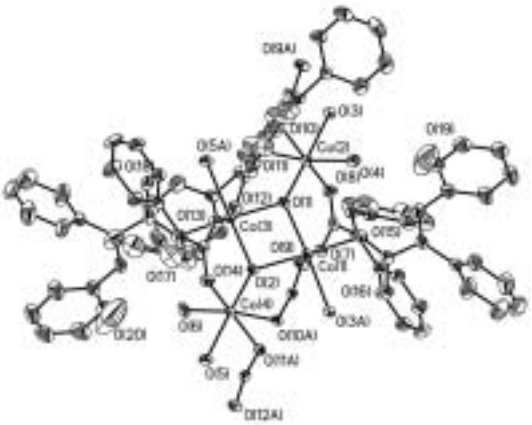

Figure 1. X-ray crystal structure of **1**.

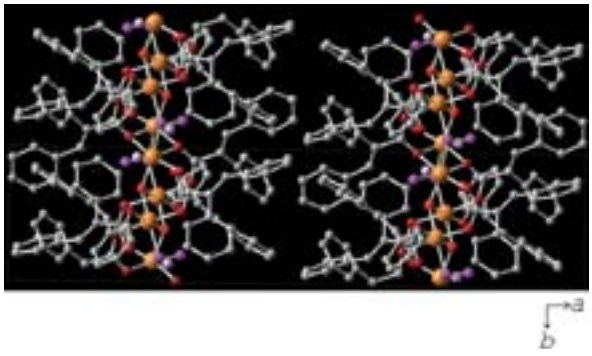

Figure 2. Packing diagram of the 1-D chain compound **1** along *c*-axis. Orange, red, dark red, purple, pink and gray represented Co, O(hydroxo), O(carboxylate), O(coordinated water), O(crystal water) and C, respectively.

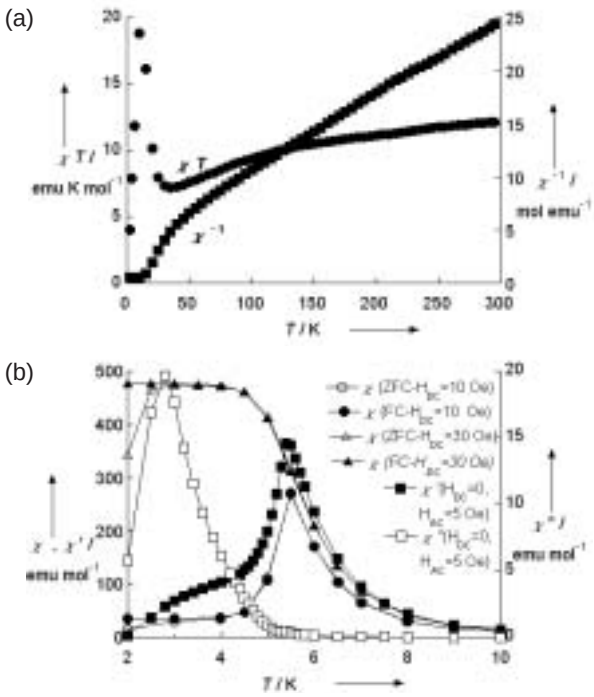

Figure 3. (a) Magnetic susceptibility of randomly oriented polycrystalline sample represented as χT and χ^{-1} per 4 Co ions. The applied field was 5 kOe. (b) Temperature dependence of the magnetic susceptibilities per 4 Co ions for oriented polycrystalline sample along *b*-axis. The applied DC field was 10 Oe and 30 Oe, and ZFC and FC refer to zero-field cooled and field-cooled, respectively. AC magnetic susceptibilities are also shown when applied DC field is 0 with AC field of 5 Oe and AC frequency of 1 Hz.

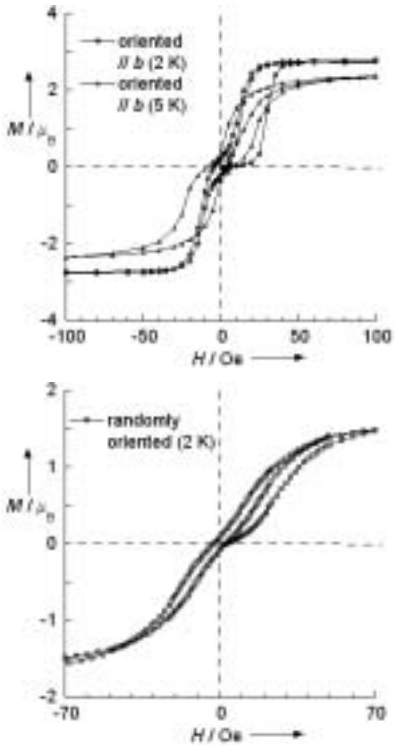

Figure 4. (a) Hysteresis loops for oriented polycrystalline sample along *b*-axis at 2 K and 5 K. (b) Hysteresis loop for randomly oriented sample at 2 K. Magnetic field was up to 70 kOe and magnetization values per 4 Co ions are shown.

V-B-2 Hydrothermal Synthesis, Structure and Magnetism of Square-Grid Cobalt(II)-Carboxylate Layered Compounds with and without Pillars

KUMAGAI, Hitoshi[1]; OKA, Yoshimi; INOUE, Katsuya; KURMOO, Mohamedally[2]
([1]IMS and Inst. Phys. Chem. Materials Strasbourg, France; [2]Inst. Phys. Chem. Materials Strasbourg, France)

[*J. Chem. Soc., Dalton Trans.* 3442–3446 (2002)]

The hydrothermal synthesis, single crystal X-ray structures and magnetic properties of two layered cobalt(II)-carboxylate complexes, $[Co^{II}(H_2O)_2(O_2C\text{-}CHCHC_6H_5)_2]$ (**1**) and $[Co^{II}(H_2O)_2(O_2CCHCHC_6H_4CO_2)_{2/2}]$ (**2**), are described. Pale red crystals of $Co(H_2O)_2L_2$, L = trans-cinnamate ($C_9H_7O_2^-$) (1) or L_2 = 4-carboxycinnamate($C_{10}H_6O_4^{2-}$) (**2**), were obtained at 120 °C. The structures consist of square-grid 2D-coordination polymeric sheets, ⋯–OCO–$Co(H_2O)_2$–OCO–$Co(H_2O)_2$–⋯, separated by C_6H_5–CH=CH– for (**1**) or pillared by –C_6H_4–CH=CH– for (**2**). (Figure 1, 2 and 3) The magnetism was studied as a function of temperature and magnetic field. In both cases the magnetic moment decreases on lowering the temperature due to spin-orbit coupling and no interaction between cobalt ions. The data can alternatively be fitted to an unrealistic quadratic layer model for S = 3/2 without taking into account the effect of spin-orbit.

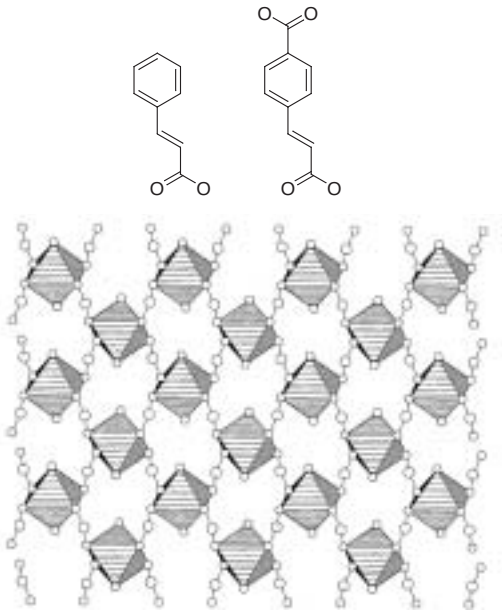

Figure 1. Crystal structure of **1** and **2** along *a* axis.

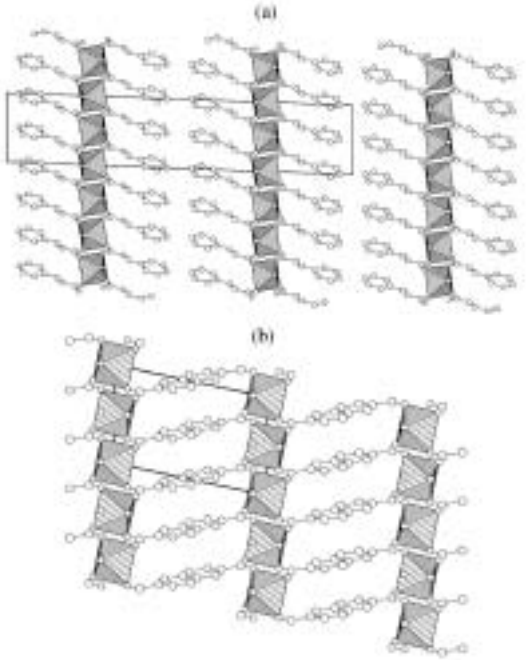

Figure 2. View of the *ab* plane arrangement of the organic backbone in the galleries in **1** (a) and **2** (b).

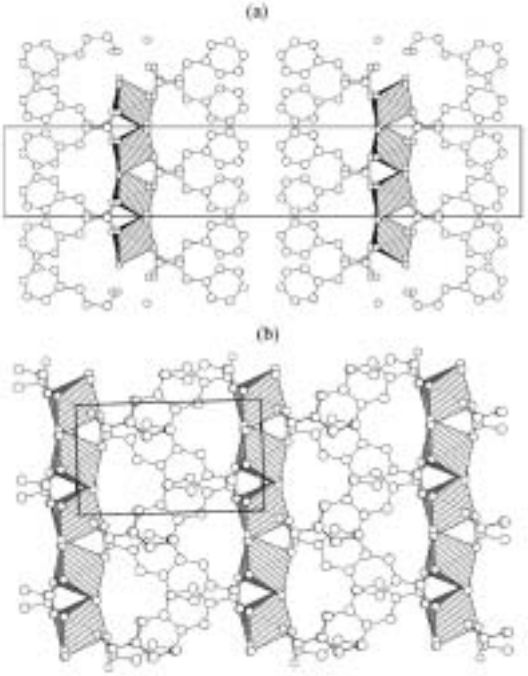

Figure 3. View of the *ac* plane arrangement of the organic backbone in the galleries in **1** (a) and **2** (b).

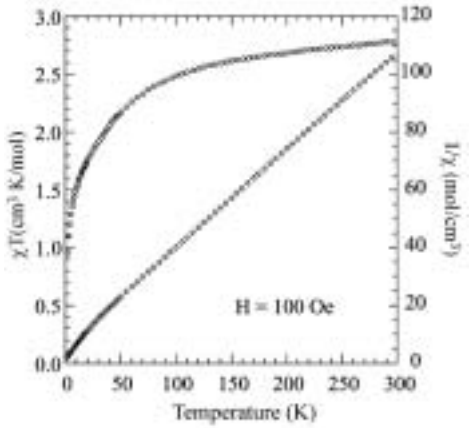

Figure 4. Temperature dependence of the product of susceptibility and temperature (circles) and the inverse susceptibility for **2** (diamonds).

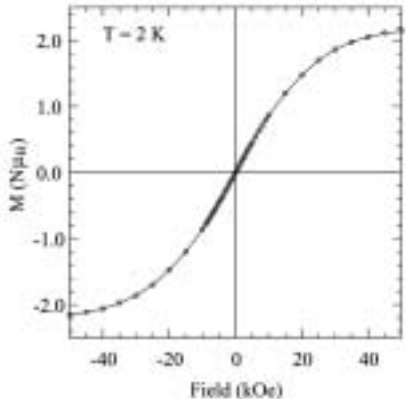

Figure 5. Isothermal magnetization of **2** at 2 K; line is a guide to the eye.

V-C Nano-Structure in Metal Oxides Prepared by Synchrotron Radiation and Swift Heavy Ions

In the project, micro-nano fabrication technique for metal oxide has been examined. The first one is the deep x-ray lithography and the liquid phase deposition method. Periodic arrangements of titanium dioxide (TiO_2) micro structure projections were fabricated in a supersaturated aqueous solution using ordered microcavities of poly(methylmethacrylate) as a template. The shape and periodicity of the TiO_2 projections were strictly controlled with the depth and arrangement of the cavities because crystalline TiO_2 was uniformly grown on the organic surface through heterogeneous nucleation. This biomimetic route is applicable to designed synthesis of three-dimensional architectures for photonic structures of various metal oxides. The other method is by using of the latent tracks introduced by the swift heavy ion. Micro structure having nano-order flatness was achieved after chemical etching. This method can be applied to create photonic crystal structure of titanium dioxide.

V-C-1 Nano/Micro-Structure in Metal Oxides Prepared by MeV Ions, Laser and Synchrotron Radiation

AWAZU, Koichi[1]; FUJIMAKI, Makoto[2]
([1]IMS and AIST; [2]AIST)

[*Handbook of Organic-Inorganic hybrid materials and Nanocomposites*, American Scientific Publishers, Chapter K, pp.1–29 (2002)]

As semiconductor device dimensions are scale down, there is also a parallel trend to minimized mechanical components and integrate these micro-mechanical components. Microelectronic devices to form micro-electro-mechanical systems (MEMS) and photonic crystals are typical examples. Especially, there has been increasing interest in photonic crystals in which the refractive index changes periodically. Various important scientific and engineering applications, such as control of spontaneous emission, sharp bending of light, trapping of photons, *etc*., may be realized by creating photonic band-gap. Recently, a few semiconductors like Si, InP, GaAs, and GaP have been shown to exhibit micrometer-size pores. However, it might be too difficult to use photonic crystals of semiconductors in the photonic network. Firstly, it is impossible to connect regular optical waveguide to semiconductor with low optical transmission loss because of the difference of refractive index. Reflection between photonic crystal of semiconductor and regular optical waveguide will cause the loss of light power. One of the most attractive application for photonic crystal is the super-prism effect. This is the reason why photonic crystal draws our attention as the substitute of arrayed wavelength grating (AWG). However, thermal expansion coefficient of semiconductor is too large to use in a conventional atmosphere. In contrast, thermal expansion coefficient in some ceramics is known as almost zero. For example, thermal expansion coefficient values of silicon, TiO_2 and $94SiO_2$:$6TiO_2$ are 7×10^{-6} /K, 7×10^{-7} /K, $\sim 0 \times 10^{-7}$ /K, respectively. In other words, photonic crystals of semiconductor must be used under constant temperature precisely controlled. Photonic crystal as well as AWG would lose the reliability when they must be used at a constant temperature. This is the second reason for why photonic crystals of semiconductor are hard to use as a photonic network device. A material having very low thermal expansion coefficient as well as a refractive index in the vicinity of 1.45 must be the best material for photonic crystal. We know that photonic crystal made of SiO_2:GeO_2 or SiO_2:TiO_2 materials would be satisfied such aspects, yet we do know little about micro (nano) fabrication technique for ceramics.

In the present review, periodic arrangements of titanium dioxide (TiO_2) micro projections were fabricated in a supersaturated aqueous solution using ordered microcavities of poly(methylmethacrylate) as a template. The shape and periodicity of the TiO_2 projections were strictly controlled with the depth and arrangement of the cavities because crystalline TiO_2 was uniformly grown on the organic surface through heterogeneous nucleation. This biomimetic route is applicable to designed synthesis of three-dimensional architectures for photonic structures of various metal oxides.

V-C-2 Structure of Latent Tracks Created by Swift Heavy Ions in Amorphous SiO_2 and Zinc Phosphate Glass

AWAZU, Koichi[1]; ROORDA, Sjoerd[2]; BREBNER, John L.[2]; ISHII, Satoshi[3]; SHIMA, Kunihiro[3]
([1]IMS and AIST; [2]Univ. Montréal; [3]Univ. Tsukuba)

[*Jpn. J. Appl. Phys.* **42**, 3950–3962 (2002)]

The structure of latent tracks introduced by swift-heavy-ion irradiation was examined on both amorphous SiO_2 and zinc phosphate glass ($68P_2O_5$:$25ZnO$:$4.5Al_2O_3$:$2.5Na_2O$). In amorphous SiO_2, the frequency of the infrared absorption assigned to the asymmetric stretching vibration of Si–O decreased with irradiation. This IR peak shift has been found to be related to the transition of normal six-membered rings of SiO_4 tetrahedra to planar three-membered rings. The high etching rate of the latent tracks is strongly related to planar three-membered rings. In the ion-irradiated zinc phosphate glass, two bridging oxygen atoms bound to a phosphorus atom turned into one bridging oxygen atom. Scission of the Zn–O bond was not observed. It was concluded that the high etching rate of the latent tracks in zinc-phosphate glass is related to P–O bond scission.

V-C-3 Structural Change Induced in TiO_2 by Swift Heavy Ions and Its Application to Three Dimensional Lithography

NOMURA, Ken-ichi[1]; NAKANISHI, Tetsuya[1]; OHKI, Yoshimichi[1]; AWAZU, Koichi[2]; FUJIMAKI, Makoto[1]; ISHII, Satoshi[3]; SHIMA, Kunihiro[3]
([1]Waseda Univ.; [2]IMS and AIST; [3]Univ. Tsukuba)

[*Phys. Rev. B* **68**, 64106 (2003)]

Rutile TiO_2 single crystal was irradiated by heavy ions with a high energy of the order of several tens of MeV. A good etching selectivity that only the irradiated surface is well etched by hydrofluoric acid is induced by the irradiation. Through X-ray diffraction and high-resolution electron microscopy, it became clear that the irradiated region lost crystallization. It is considered that this amorphous region and the surrounding region are dissolved in hydrofluoric acid. Through calculation of ion energy, it was found that the etching always stopped at the depth where the electronic stopping power of the ion decayed to a critical value of 6.2 keV/nm, regardless of the ion species in the case of I, Br, Cu, and Ti ions. However, in the case of Ca ions with energies higher than about 72 MeV or Cl ions with energies higher than about 77 MeV, the irradiated top surface was not etched with the hydrofluoric acid, but the inside several μm deep from the irradiated surface was etched. A calculation shows that the critical factor which determines whether the irradiated surface can be etched or not is the lateral energy density on the surface deposited by ions. The etched surface observed by atomic force microscopy is very smooth with a roughness of the order of nm. Therefore, combination of ion irradiation and etching can be used as a novel fabrication method of nanostructures in rutile.

V-C-4 Strained Si–O–Si Bonds in Amorphous SiO_2 Materials

AWAZU, Koichi[1]; KAWAZOE, Hiroshi[2]
([1]IMS and AIST; [2]Hoya Corp.)

[*J. Appl. Phys.* **94**, 6243 (2003)]

Amorphous SiO_2 (*a*-SiO_2), such as bulk silica glasses and thin films has been one of the key materials in modern opto-electronic industries. These materials are currently used in communication technologies as optical fibers, thin films for electrical insulation in dynamic random access memories (DRAM), and optical lenses for excimer laser lithography, for example. The property essential for these applications is the wide band gap amounting to ~ 9 eV. However, bulk silica glasses commercially available and silica thin films show photo-responses to sub-band gap lights in the vicinity of 5 eV and unexpected trapping of charges, and the behavior has a strong dependency on the preparation history.

A number of studies were carried out to clarify the relationship between the properties and structural imperfections in the materials and the formation mechanisms of the defects. There are two categories of the imperfections: one is dopant- or impurity-related imperfections and the other is non-stoichiometry related defects. These defects constitute gap states in *a*-SiO_2. The structural identification was usually performed by absorption- and emission spectroscopy in the visible-ultraviolet region and electron spin resonance (ESR). The experimentally proposed models were compared with the predictions by theoretical calculations of energy levels.

Recent development of the excimer laser lithography technique led us to recognize that a latent member, which has been unnoticed because of no response to the optical absorption or emission in the visible-uv range and ESR absorption, exists in the family of active centers in *a*-SiO_2, that is a strained Si–O–Si bond originating from the planar three membered ring. In contrast, the puckered four membered ring is unstrained. Although it has been pointed out that there was a wide distribution in Si–O–Si bond angle from 90° to 180° by X-ray analysis or ^{29}Si solid state NMR, the physical and chemical responses of the Si–O–Si bonds with a particular bond angle could not be differentiated.

Very recently it was clarified that a strained Si–O–Si bond, in other words chemically excited bonds, has an optical absorption locating on the band edge. The chemically excited bond can be scavenged by fluorine doping, because it is chemically reactive. In the present review we show that the unresolved optical and electric responses of silica glasses can be comprehensively understood by taking the presence of the strained bonds into consideration.

V-D Structures and Properties of Lanthanoid-Metallofullerenes

Lanthanoid-containing metallofullerenes with C_{82} cages, M@C_{82} (M is a lanthanoid metal atom), are the most widely investigated metallofullerenes. Accordingly to the oxidation state of the metal atom inside, they are classified into two groups; in one the metal atom takes the divalent state, and in the other it takes the trivalent state. Recently we investigated the cage structures and the motions of endohedral metal in metallofullerenes of the former group by ^{13}C NMR spectroscopy.

V-D-1 Structural Study of Four Ca@C_{82} Isomers by ^{13}C NMR Spectroscopy

KODAMA, Takeshi[1]; FUJII, Ryosuke[1]; MIYAKE, Yoko[1]; SAKAGUCHI, Koichi[1]; NISHIKAWA, Hiroyuki[1]; IKEMOTO, Isao[1]; KIKUCHI, Koichi[2]; ACHIBA, Yohji[1]
([1]Tokyo Metropolitan Univ.; [2]IMS and Tokyo Metropolitan Univ.)

[*Chem. Phys. Lett.* **377**, 197 (2003)]

The ^{13}C NMR spectra of four Ca@C_{82} isomers have been measured. The symmetry of isomers I, II, III and IV are assigned to be C_s, C_{3v}, C_2 and C_{2v}, respectively. For isomer IV, the cage is specified to be $C_{2v}(9)$. Our experimental results regarding the symmetry of cage structure coincide with the theoretical predictions.

V-E Development of Organic Superconductors

Since the discovery of superconductivity in a series of salts of TMTSF, TCF (tetrachalcogenafulvalene) derivatives have served as π-electron donors for the development of new organic superconductors. Although considerable research effort in this field has focused on the construction of TCF-type donors with extended π-conjugation, these donors, except for the DTEDT donor, failed to yield any organic superconductors. Besides TCF derivatives, our reported BDA-TTP donor gives three superconducting salts. And we succeeded in developing two superconductors from DODHT, with a less extended π-system that that of TCF derivatives. Recently other superconductors have been produced from these donors.

V-E-1 A New Organic Superconductor, $(DODHT)_2BF_4H_2O$

NISHIKAWA, Hiroyuki[1]; MACHIDA, Asami[1]; MORIMOTO, Takanobu[1]; KIKUCHI, Koichi[2]; KODAMA, Takeshi[1]; IKEMOTO, Isao[1]; YAMADA, Jun-ichi[3]; YOSHINO, Harukazu[4]; MURATA, Keizo[4]
([1]Tokyo Metropolitan Univ.; [2]IMS and Tokyo Metropolitan Univ.; [3]Himeji Inst. Tech.; [4]Osaka City Univ.)

[*Chem. Commun.* 494 (2003)]

In addition to two organic superconductors $(DODHT)_2X$ [DODHT = (1,4-dioxane-2,3-diyldithio)-dihydro-tetrathiafulvalene; X = PF_6 and AsF_6] previously reported by us, the BF_4 salt of DODHT containing one water molecule [$(DODHT)_2BF_4H_2O$] has been found to undergo a superconducting transition at 3.2 K under a hydrostatic pressure of 15.5 kbar.

V-E-2 A New Organic Superconductor, β-$(BDA\text{-}TTP)_2GaCl_4$ [BDA-TTP = 2,5-(1,3-Dithian-2-Ylidene)-1,3,4,6-Tetrathiapentalene]

YAMADA, Jun-ichi[1]; TOITA, Takashi[1]; AKUTSU, Hiroki[1]; NAKATSUJI, Shin'ichi[1]; NISHIKAWA, Hiroyuki[2]; IKEMOTO, Isao[2]; KIKUCHI, Koichi[3]; CHOI, Eun S.[4]; GRAF, David[4]; BROOKS, James S.[4]
([1]Himeji Inst. Tech.; [2]Tokyo Metropolitan Univ.; [3]IMS and Tokyo Metropolitan Univ.; [4]Florida State Univ.)

[*Chem. Commun.* 2230 (2003)]

The preparation, crystal structure and physical properties of β-$(BDA\text{-}TTP)_2GaCl_4$ has been investigated; the salt exhibits superconductivity at 3.1 K (onset) under a hydrostatic pressure of 7.6 kbar.